

Implementation of Voltage Sag Relative Location and Fault Type Identification Algorithm Using Real-Time Distribution System Data

Yalman, Yunus; Uyanık, Tayfun; Tan, Adnan; Bayındır, Kamil Çağatay; Terriche, Yacine; Su, Chun Lien; Guerrero, Josep M.

Published in:
Mathematics

DOI (link to publication from Publisher):
[10.3390/math10193537](https://doi.org/10.3390/math10193537)

Creative Commons License
CC BY 4.0

Publication date:
2022

Document Version
Publisher's PDF, also known as Version of record

[Link to publication from Aalborg University](#)

Citation for published version (APA):

Yalman, Y., Uyanık, T., Tan, A., Bayındır, K. Ç., Terriche, Y., Su, C. L., & Guerrero, J. M. (2022). Implementation of Voltage Sag Relative Location and Fault Type Identification Algorithm Using Real-Time Distribution System Data. *Mathematics*, 10(19), Article 3537. <https://doi.org/10.3390/math10193537>

General rights

Copyright and moral rights for the publications made accessible in the public portal are retained by the authors and/or other copyright owners and it is a condition of accessing publications that users recognise and abide by the legal requirements associated with these rights.







- Users may download and print one copy of any publication from the public portal for the purpose of private study or research.
- You may not further distribute the material or use it for any profit-making activity or commercial gain
- You may freely distribute the URL identifying the publication in the public portal -

Take down policy

If you believe that this document breaches copyright please contact us at vbn@aub.aau.dk providing details, and we will remove access to the work immediately and investigate your claim.

Article

Implementation of Voltage Sag Relative Location and Fault Type Identification Algorithm Using Real-Time Distribution System Data

Yunus Yalman ¹, Tayfun Uyanık ², Adnan Tan ³, Kamil Çağatay Bayındır ¹, Yacine Terriche ⁴, Chun-Lien Su ^{5,*} and Josep M. Guerrero ⁴

¹ Department of Electrical and Electronic Engineering, Ankara Yıldırım Beyazıt University, Ankara 06010, Turkey

² Maritime Faculty, Istanbul Technical University, Istanbul 34940, Turkey

³ Department of Electrical and Electronics Engineering, Çukurova University, Adana 01250, Turkey

⁴ Center for Research on Microgrids, AAU Energy, 9220 Aalborg, Denmark

⁵ Department of Electrical Engineering, National Kaohsiung University of Science and Technology, Kaohsiung City 807618, Taiwan

* Correspondence: cls@nku.edu.tw

Abstract: One of the common power quality (PQ) problems in transmission and distribution systems is the voltage sag that affects the sensitive loads. Losses and problems caused by the voltage sag in the power system can be reduced by correctly determining the relative location of the voltage sag. This paper proposes a novel algorithm to classify voltage sag relative location and fault type, which is the main root cause of voltage sag, based on the actual voltage and current data before and during the voltage sag. The performance of the algorithm is investigated by performing a numerical simulation utilizing MATLAB/Simulink. Moreover, the proposed algorithm is integrated into the power quality monitoring system (PQMS) of the real distribution system and tested. The results show that the performance of the proposed method is satisfactory.

Keywords: distribution system; fault type; power quality; voltage sag

MSC: 90C90



Citation: Yalman, Y.; Uyanık, T.; Tan, A.; Bayındır, K.Ç.; Terriche, Y.; Su, C.-L.; Guerrero, J.M. Implementation of Voltage Sag Relative Location and Fault Type Identification Algorithm Using Real-Time Distribution System Data. *Mathematics* **2022**, *10*, 3537. <https://doi.org/10.3390/math10193537>

Academic Editors: Denis N. Sidorov and Pantelis Sopasakis

Received: 30 August 2022

Accepted: 23 September 2022

Published: 28 September 2022

Publisher's Note: MDPI stays neutral with regard to jurisdictional claims in published maps and institutional affiliations.



Copyright: © 2022 by the authors. Licensee MDPI, Basel, Switzerland. This article is an open access article distributed under the terms and conditions of the Creative Commons Attribution (CC BY) license (<https://creativecommons.org/licenses/by/4.0/>).

1. Introduction

Voltage sag, a decrease in the magnitude of voltage to between 0.1 pu and 0.9 pu for a period from 0.5 cycles to one minute and can be defined “two-dimensional” power quality event, is a vital PQ problem in distribution and transmission systems [1]. These “two-dimensional” PQ events are explained as the minimum value/total time approach [2]. According to statistical data, more than 80% of complaints about PQ are voltage sag [3]. In the industrial production process, there are sensitive loads, equipment, and digital automatic control systems. Compared with conventional systems, voltage sag easily affects these sensitive systems. Even if the normal operation of these systems may be affected by a few cycles of voltage sag, which is concluded with tripping or malfunction of the device, and it causes immeasurable economic losses. However, both utilities and customer are responsible for PQ. Due to the absence of a correct assessment of the reasons for PQ deteriorating, conflict arises between the power suppliers and consumers. Hence, determining voltage location is important for researchers [4–8]. After voltage sag location is detected, a mitigation strategy can be fulfilled. Theoretically, the information related to protection systems for short circuit currents could figure out the problem. Correlating sag start times, durations and duration of intervention of the protection systems can determine the location of voltage sag. However, this cannot apply in the actual distribution or transmission networks. Even if it can be done, correctness is insufficient because of

measurement error and the absence of precise synchronization between the measurement times. Moreover, due to operating the transmission and distribution by different operators, their measurements are not shared and exchanged by operators. Thus, correlation is not possible [9]. Moreover, it causes many disagreements between the transmission system operator (TSO) and distribution system operator (DSO) in deciding on the responsibilities and determining financial penalties [10].

Locating the voltage sag source is to decide on which side of a PQ monitoring device the voltage sag originates. Many papers have been published in the literature on the subject of defining voltage sag location. In [11], relative voltage sag location is determined using power and energy methods. In [12], instantaneous active and reactive energy can classify the origin of voltage sag. However, instantaneous active and reactive energy can be affected by the fault type and the distributed generation unit (DG) type. In [13], the polarity of the voltage-current slope determines voltage sag location. If the sign of this slope is negative, the location of the voltage sag is classified as downstream (DS), and if the sign of this slope is positive, the location of the voltage sag is classified as upstream (US). In [14], a novel method is proposed based on the direction of the real current component at starting of the fault. If the real current component is positive, the origin of the voltage sag is from downstream (DS). If the real current component is not positive, the source of the voltage sag is from upstream. The proposed algorithm is convenient for a radial distribution system. In [15], a new current-based algorithm is proposed for determining the location of voltage sag by using directional overcurrent relay (DOC) information based on a change in magnitude of positive-sequence current and phase-angle jump. In [16], the origin of voltage sag is determined by using only line current measurements, which is an instantaneous vector-based method. In this method, the instantaneous current vector is converted to Clarke's- $\alpha\beta$ component to define the relative voltage sag location. Ref. [17] proposes a novel approach to determine the origin of voltage sag dependent on magnitude and phase change in the instantaneous positive-sequence current. When compared with phasor-based method, it shows faster response, high accuracy for the grid with distributed generation, and active loads. The location of voltage sag is determined by using only voltage measurements [18,19]. The polarity of the fundamental positive sequence resistance determined at a metering point is used as an indicator to find out the origin of voltage sag. The resistance is calculated by using the least-squares method [20]. The voltage sag location is detected by the sign of the real part of internal impedance in two single-port networks. If the real part of the internal impedance is positive, the voltage sag location is classified as downstream; if the real part of the internal impedance is negative, the voltage sag location is classified upstream [6]. In [10], the new method is proposed based on the DOC information using change in positive-sequence current and its phase angle jump. In [21], the new current-based method obtained by improving [9], which uses controller parameters of inverter and positive sequence power factor, is proposed for an active distribution system with the presence of an inverter-based generation system. In [22], a novel method, which uses the ratio of current magnitude and variation of positive sequence power factor component, is introduced during the sag and presage to define relative voltage sag location at the point of common coupling of constant loads.

In the literature, different methods related to artificial intelligence and statistical, which are support vector machine [23,24], multivariable regression method [25,26], artificial neural network [27], deep learning method [28,29], AdaBoost algorithm [30], Attention-based Recurrent Neural Network [31], pattern recognition [32], multi-label random forest algorithm [33], are implemented to find the relative voltage sag location.

In this paper, the voltage sag location is classified as DS or US, and after determination of voltage sag location, fault type is defined as a single-phase ground fault (SLGP), two-phase ground fault (LLGF), three-phase ground fault (LLLGF), and two-phase fault (LLF). Moreover, the novel algorithm is integrated into Inavitas [34] which is the most common PQMS used at distribution system companies in Turkey. The performance of the proposed method is approved by utilizing actual event data recorded by PQMS and simulation study.

The results indicate that the proposed algorithm detects voltage sag location with high accuracy regardless of uncertainty related to distribution system parameters.

The main contributions of the present work can be summarized as follows:

- This paper proposes a novel algorithm to determine voltage sag location and fault type using voltage and current magnitude before and during the voltage sag recorded by PQMS in the actual distribution system company.
- The proposed algorithm is integrated into PQMS, making it valuable for engineering applications. Moreover, it can help the solving disagreement regarding voltage sag location between different operators.

This paper is organized as follows: In Section 1, the introduction is given. In Section 2, the proposed algorithm is explained. Simulation results are discussed in Section 3. Finally, Section 4 provides the conclusions of this work, and future works are mentioned.

1.1. Problem Definition

Determining the location of the voltage sag helps system operators to take fast action to mitigate PQ problems in transmission and distribution systems. System operators can access the data recorded during the voltage sag through PQMS. This paper aims to determine the relative location of voltage sag and fault type with limited data (current and voltage magnitudes during and before the voltage sag) provided by PQMS of a real distribution system. Moreover, the proposed method should be suitable for real-time applications as it will be integrated into the PQMS of the distribution system.

1.2. Problem Solution

PQMS provides voltage and current magnitude during and before the voltage sag recorded by the PQ analyzer. The rule-based algorithm is developed using these data to determine voltage sag relative location and fault type. The developed algorithm is integrated into the PQMS of the distribution system and tested. Moreover, the performance of the algorithm is investigated with numerical simulation.

2. Proposed Method

The new algorithm is proposed to determine voltage sag location based on a voltage and current magnitude change during and before sag using actual event data recorded by PQMS. Moreover, this algorithm is implemented and tested on Inavitas software PQMS used by most distribution companies in Turkey. A general overview of the proposed system and an example of voltage sag data provided by PQMS is shown in Figure 1. When a voltage sag occurs in the distribution system, PQMS provides three-phase current and voltage magnitude data before and during the voltage sag, duration of voltage sag, event time, and the nominal voltage of the bus via the PQ analyzer. The proposed algorithm classifies the location of voltage sag as US or DS. If the origin of the voltage sag is DS, then the fault type that causes voltage sag is determined.

The flowchart diagram of the proposed algorithm is shown in Figure 2. As can be seen from the flowchart diagram, firstly, the voltage sag data is processed by eliminating some event data regarding measurement error, absence of current measurement, and interruption event. Secondly, the proposed algorithm determines the voltage sag location based on the total score of each voltage sag event, which is calculated by the scoring algorithm shown in Figure 3. If the voltage sag location is detected as a DS, the fault type is classified using the fault type algorithm demonstrated in Figure 4. Total score can be expressed as in Equation (1).

$$TS_t = \sum_{i=1}^{26} S_i \quad (1)$$

where S_i is a score of the voltage sag event that satisfies the i -th rule, " i " index represents the rule number, and TS_t is total score. The voltage and current data of the phases which are $V_{1\max}$, $V_{1\min}$, $V_{2\max}$, $V_{2\min}$, $V_{3\max}$, $V_{3\min}$, $I_{1\max}$, $I_{1\min}$, $I_{2\max}$, $I_{2\min}$, $I_{3\max}$, $I_{3\min}$ are read from the database where $V_{p\max}$ is the voltage magnitude during the voltage sag, $V_{p\min}$

is the voltage magnitude before the voltage sag, I_{pmax} is the current magnitude during the voltage sag. I_{pmin} is current magnitude during the voltage sag. The C_p and MC_p is calculated using Equations (2) and (3), respectively.

$$C_1 = \frac{I_{1max}}{I_{1min}}, C_2 = \frac{I_{2max}}{I_{2min}}, C_3 = \frac{I_{3max}}{I_{3min}} \quad (2)$$

$$MC_1 = \frac{I_{1max}}{I_{2max}}, MC_2 = \frac{I_{1max}}{I_{3max}}, MC_3 = \frac{I_{2max}}{I_{1max}}, MC_4 = \frac{I_{2max}}{I_{3max}}, MC_5 = \frac{I_{3max}}{I_{1max}}, MC_6 = \frac{I_{3max}}{I_{2max}} \quad (3)$$

where p is phase number, C_p is the proportion of maximum current to the minimum current during the voltage sag for phase, MC_p is the proportion of maximum current to the maximum current during the voltage sag for different phases. The MV_1 , MV_2 , and MV are given by expressions (4)–(6), respectively.

$$MV_1 = \max(V_{1max}, V_{2max}, V_{3max}) \quad (4)$$

$$MV_2 = \min(V_{1min}, V_{2min}, V_{3min}) \quad (5)$$

$$MV = MV_1 - MV_2 \quad (6)$$

where MV_1 shows the biggest value of maximum voltages for three phases, MV_2 is the smallest value of minimum voltages for three phases, and MV represents the difference between the MV_1 and MV_2 .

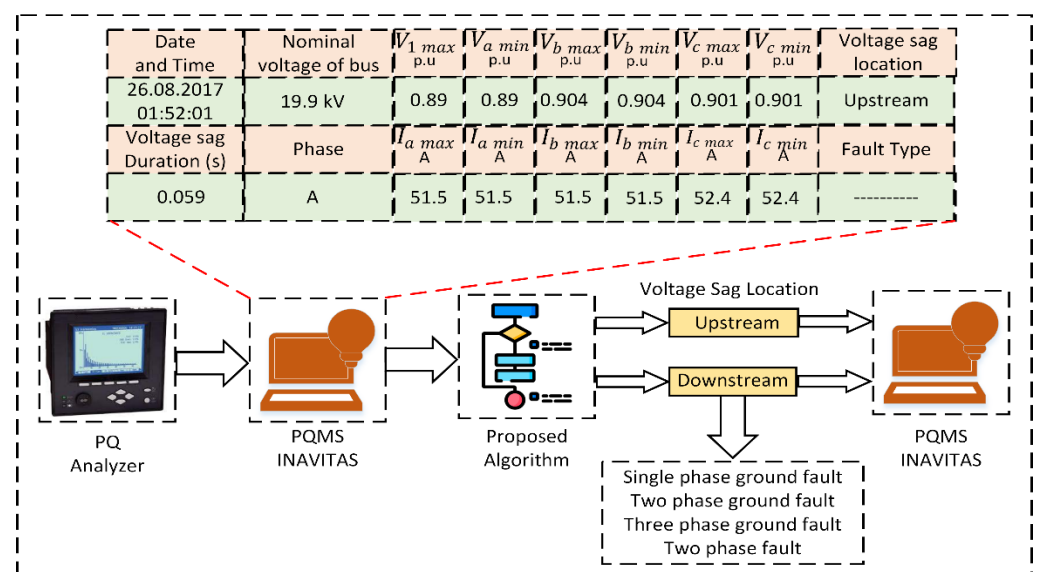


Figure 1. General overview of the proposed method.

2.1. Scoring Algorithm

A rule-based algorithm is developed to determine voltage sag location and fault type based on the voltage and current change before and during the voltage sag. The flowchart diagram of the algorithm is demonstrated in Figure 3. After reading voltage sag data from the database, the D_i is calculated using rules shown in Table 1 and the C_p , MV , and MC_p is computed utilizing Equations (2)–(6). Each rule given in Table 2 is checked one by one, and the total score (TS_i) is calculated according to the conditions provided. If the TS_i is bigger than 6, the direction of voltage sag is DS; otherwise, it is the US.

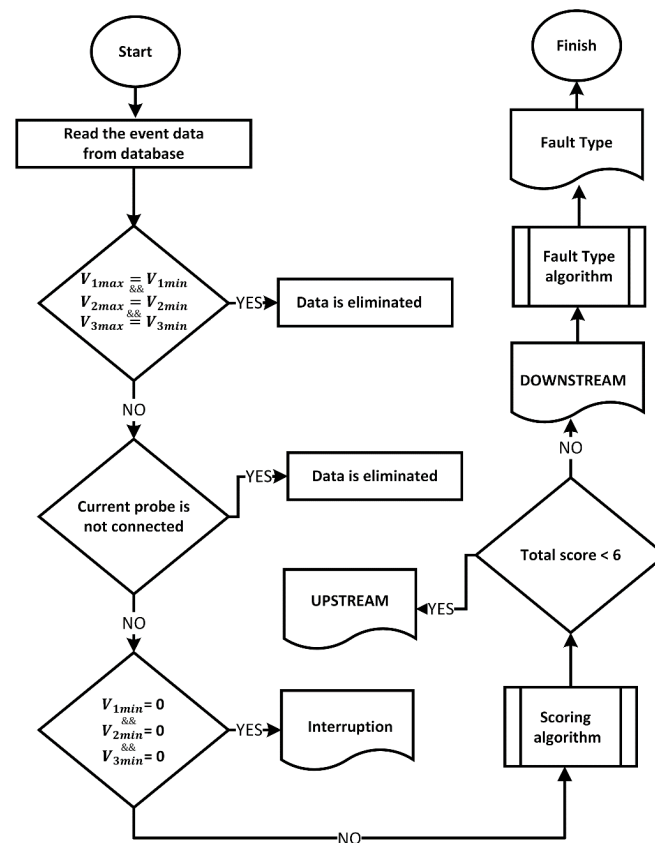


Figure 2. Flowchart diagram of the proposed method.

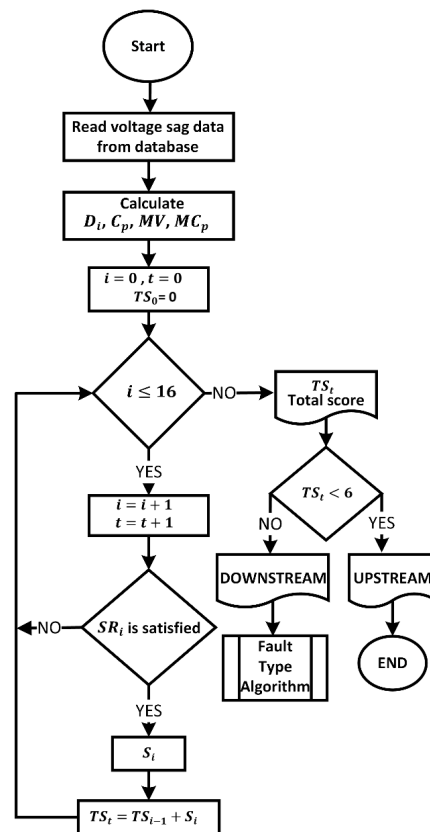


Figure 3. Flow diagram of the scoring algorithm.

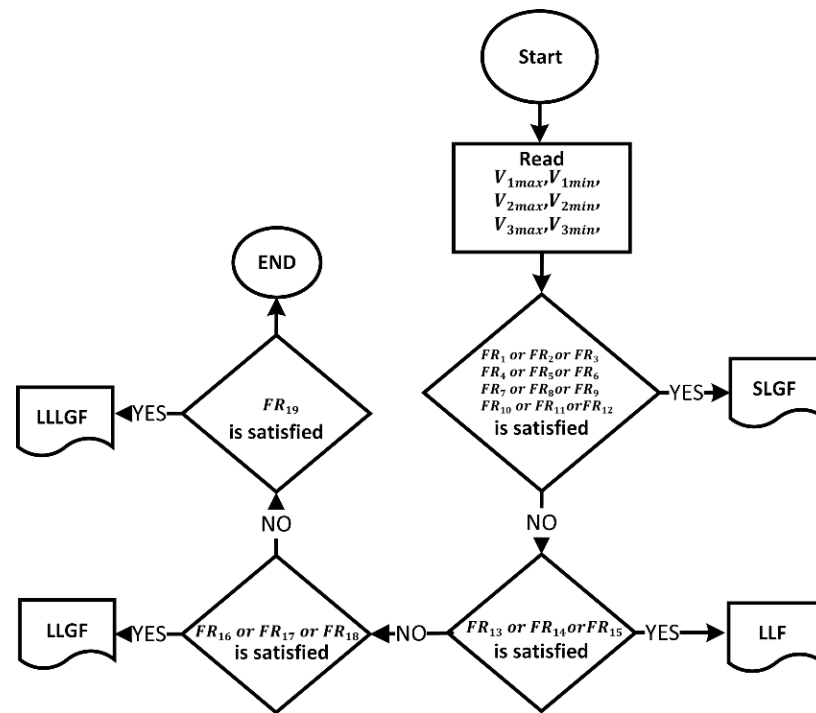


Figure 4. Flowchart diagram of fault type algorithm.

Table 1. Rules of the scoring algorithm.

Rule 1: if ($V_{1min} \leq 0.9$ and $V_{2max} \geq 1.1$ and $V_{3min} > 0.9$ and $V_{3max} < 1.1$) then $D_1 = V_{3min} - V_{1min}$, $D_2 = V_{2max} - V_{3max}$
Rule 2: if ($V_{1min} \leq 0.9$ and $V_{2max} < 1.1$ and $V_{2min} > 0.9$ and $V_{3max} \geq 1.1$) then $D_1 = V_{2min} - V_{1min}$, $D_2 = V_{3max} - V_{2max}$
Rule 3: if ($V_{1min} > 0.9$ and $V_{1max} < 1.1$ and $V_{2min} \leq 0.9$ and $V_{3max} \geq 1.1$) then $D_1 = V_{1min} - V_{2min}$, $D_2 = V_{3max} - V_{1max}$
Rule 4: if ($V_{1min} > 0.9$ and $V_{1max} < 1.1$ and $V_{2max} \geq 1.1$ and $V_{3min} \leq 0.9$) then $D_1 = V_{1min} - V_{3min}$, $D_2 = V_{2max} - V_{1max}$
Rule 5: if ($V_{1max} \geq 1.1$ and $V_{2min} \leq 0.9$ and $V_{3min} > 0.9$ and $V_{3max} < 1.1$) then $D_1 = V_{3min} - V_{2min}$, $D_2 = V_{1max} - V_{3max}$
Rule 6: if ($V_{1max} \geq 1.1$ and $V_{2min} > 0.9$ and $V_{2max} < 1.1$ and $V_{3min} < 0.9$) then $D_1 = V_{2min} - V_{3min}$, $D_2 = V_{1max} - V_{2max}$
Rule 7: if ($V_{1min} \leq 0.9$ and $V_{2min} > 0.9$ and $V_{2max} < 1.1$ and $V_{3min} > 0.9$ and $V_{3max} < 1.1$) then $D_1 = V_{3min} - V_{1min}$, $D_2 = V_{2min} - V_{1min}$
Rule 8: if ($V_{1min} > 0.9$ and $V_{1max} < 1.1$ and $V_{2min} \leq 0.9$ and $V_{3min} > 0.9$ and $V_{3max} < 1.1$) then $D_1 = V_{3min} - V_{2min}$, $D_2 = V_{1min} - V_{2min}$
Rule 9: if ($V_{1min} > 0.9$ and $V_{1max} < 1.1$ and $V_{2min} \leq 0.9$ and $V_{3min} > 0.9$ and $V_{3max} < 1.1$) then $D_1 = V_{2min} - V_{3min}$, $D_2 = V_{1min} - V_{3min}$
Rule 10: if ($V_{1min} \leq 0.9$ and $V_{2max} \geq 1.1$ and $V_{3max} \geq 1.1$) then $D_1 = V_{1min} - 0.9$, $D_2 = V_{2max} - 1.1$, $D_3 = V_{3max} - 1.1$
Rule 11: if ($V_{1max} \geq 1.1$ and $V_{2min} \leq 0.9$ and $V_{3max} \leq 1.1$) then $D_1 = V_{1max} - 1.1$, $D_2 = V_{2min} - 0.9$, $D_3 = V_{3max} - 1.1$
Rule 12: if ($V_{1max} \geq 1.1$ and $V_{2max} \geq 1.1$ and $V_{3min} \leq 0.9$) then $D_1 = V_{1max} - 1.1$, $D_2 = V_{2max} - 1.1$, $D_3 = V_{3min} - 0.9$
Rule 13: if ($V_{1min} \leq 0.9$ and $V_{2min} \leq 0.9$ and $V_{3max} < 1.1$ and $V_{3min} > 0.9$) then $D_1 = V_{3min} - V_{1min}$, $D_2 = V_{3min} - V_{2min}$
Rule 14: if ($V_{1min} \leq 0.9$ and $V_{2min} > 0.9$ and $V_{2max} < 1.1$ and $V_{3min} \leq 0.9$) then $D_1 = V_{2min} - V_{1min}$, $D_2 = V_{2min} - V_{3min}$
Rule 15: if ($V_{1min} > 0.9$ and $V_{1max} < 1.1$ and $V_{2min} \leq 0.9$ and $V_{3min} \leq 0.9$) then $D_1 = V_{1min} - V_{2min}$, $D_2 = V_{1min} - V_{3min}$
Rule 16: if ($V_{1min} \leq 0.9$ and $V_{2min} \leq 0.9$ and $V_{3max} \geq 1.1$) then $D_1 = V_{1min} - 0.9$, $D_2 = V_{2min} - 0.9$, $D_3 = V_{3max} - 1.1$
Rule 17: if ($V_{1min} \leq 0.9$ and $V_{2max} \geq 1.1$ and $V_{3min} \leq 0.9$) then $D_1 = V_{1min} - 0.9$, $D_2 = V_{2max} - 1.1$, $D_3 = V_{3min} - 0.9$
Rule 18: if ($V_{1max} \geq 1.1$ and $V_{2min} \leq 0.9$ and $V_{3min} \leq 0.9$) then $D_1 = V_{1min} - 0.9$, $D_2 = V_{2max} - 1.1$, $D_3 = V_{3min} - 0.9$
Rule 19: if ($V_{1min} \leq 0.9$ and $V_{2min} \leq 0.9$ and $V_{3min} \leq 0.9$) then $D_1 = V_{1min} - 0.9$, $D_2 = V_{2min} - 0.9$, $D_3 = V_{3min} - 0.9$
Rule 20: if ($V_{1max} \geq 1.1$ and $V_{2min} > 0.9$ and $V_{2max} < 1.1$ and $V_{3min} > 0.9$ and $V_{3max} < 1.1$) then $D_1 = V_{1max} - V_{2max}$, $D_2 = V_{1max} - V_{3max}$
Rule 21: if ($V_{1min} > 0.9$ and $V_{1max} < 1.1$ and $V_{2max} \geq 1.1$ and $V_{3min} > 0.9$ and $V_{3max} < 1.1$) then $D_1 = V_{2max} - V_{1max}$, $D_2 = V_{2max} - V_{3max}$
Rule 22: if ($V_{1min} > 0.9$ and $V_{1max} < 1.1$ and $V_{2max} < 1.1$ and $V_{2min} > 0.9$ and $V_{3max} \geq 1.1$) then $D_1 = V_{3max} - V_{1max}$, $D_2 = V_{3max} - V_{2max}$
Rule 23: if ($V_{1max} \geq 1.1$ and $V_{2max} \geq 1.1$ and $V_{3min} > 0.9$ and $V_{3max} < 1.1$) then $D_1 = V_{1max} - V_{3max}$, $D_2 = V_{2max} - V_{3max}$
Rule 24: if ($V_{1max} \geq 1.1$ and $V_{2max} < 1.1$ and $V_{2min} > 0.9$ and $V_{3max} \geq 1.1$) then $D_1 = V_{1max} - V_{2max}$, $D_2 = V_{3max} - V_{2max}$
Rule 25: if ($V_{1min} > 0.9$ and $V_{1max} < 1.1$ and $V_{2max} \geq 1.1$ and $V_{3max} \geq 1.1$) then $D_1 = V_{2max} - V_{1max}$, $D_2 = V_{3max} - V_{1max}$
Rule 26: if ($V_{1max} \geq 1.1$ and $V_{2max} \geq 1.1$ and $V_{3max} \geq 1.1$) then $D_1 = V_{1max} - 1.1$, $D_2 = V_{2max} - 1.1$, $D_3 = V_{3max} - 1.1$

2.2. Fault Type Identification

The rule-based fault type identification algorithm is developed. The flowchart diagram of the algorithm is indicated in Figure 4. After the voltage sag relative location is determined as a DS, the fault type, which is the main reason for voltage sag, is classified as SLGF, LLGF, LLLGF, and LLF. Table 3 demonstrates rules that are used to classify the fault type. When one of the rules is satisfied, the fault type is classified.

Table 2. Rules of the scoring algorithm.

SR ₁ : if ($D_1 \geq 0.5$ or $D_2 \geq 0.5$) then $S_i = 5$
SR ₂ : if ($0.3 \geq D_1 > 0.2$ or $0.3 \geq D_2 > 0.2$) then $S_i = 3$
SR ₃ : if ($0.2 \geq D_1 > 0.1$ or $0.2 \geq D_2 > 0.1$) then $S_i = 2$
SR ₄ : if ($0.1 \geq D_1 > 0$ or $0.1 \geq D_2 > 0$) then $S_i = 1$
SR ₅ : if ($D_1 \geq 0.5$ or $D_2 \geq 0.5$ or $D_3 \geq 0.5$) then $S_i = 5$
SR ₆ : if ($0.3 \geq D_1 > 0.2$ or $0.3 \geq D_2 > 0.2$ or $0.3 \geq D_3 > 0.2$) then $S_i = 3$
SR ₇ : if ($0.2 \geq D_1 > 0.1$ or $0.2 \geq D_2 > 0.1$ or $0.2 \geq D_3 > 0.1$) then $S_i = 2$
SR ₈ : if ($0.1 \geq D_1 > 0$ or $0.1 \geq D_2 > 0$ or $0.1 \geq D_3 > 0$) then $S_i = 1$
SR ₉ : if ($(V_{1\max} - V_{1\min} \leq 0.02)$ and $(V_{2\max} - V_{2\min} \leq 0.02)$ and $(V_{3\max} - V_{3\min} \leq 0.02)$) then $S_i = -5$
SR ₁₀ : if ($MV > 0.5$) then $S_i = 5$
SR ₁₁ : if ($0.5 > MV > 0.4$) then $S_i = 4$
SR ₁₂ : if ($0.4 > MV > 0.3$) then $S_i = 3$
SR ₁₃ : if ($0.3 > MV > 0.2$) then $S_i = 2$
SR ₁₄ : if ($MV < 0.2$) then $S_i = 0$
SR ₁₅ : if ($C_1 > 1.3$ or $C_2 > 1.3$ or $C_3 > 1.3$) and if ($C_1 > 5$ and $C_2 > 5$ and $C_3 > 5$) then $S_i = 5$
SR ₁₆ : if ($C_1 > 1.3$ or $C_2 > 1.3$ or $C_3 > 1.3$) then $S_i = 4$
SR ₁₇ : if ($MC_1 > 1.3$ or $MC_2 > 1.3$ or $MC_3 > 1.3$ or $MC_4 > 1.3$ or $MC_5 > 1.3$ or $MC_6 > 1.3$) then $S_i = 4$

2.3. Implementation of the Proposed Algorithm into PQMS

Firstly, the proposed algorithm has been tested in Matlab. After that, the algorithm has been implemented in PQMS. The result of the algorithm is also confirmed with voltage and current waveform recorded by the PQ analyzer. A total of 6140 voltage sag events are examined. 5825 of the events are the US, and 315 events are the DS. 79 of DS events are LLGF, 207 of DS events are SLGF, and 29 of DS events are LLLGF. Data regarding voltage sag event and algorithm results shown by PQMS is demonstrated in Table 4 as an example. While the event direction and fault type are determined by the proposed method, the current and voltage waveform is provided by the PQ analyzer for voltage sag. Each result is explained in detail below:

- For events 1–4, the algorithm determines the voltage sag relative location as a DS, and fault type is classified as SFGL. When the current and voltage waveforms shown in Figures A1–A4 are investigated, a voltage sag has occurred in one phase, and overcurrent is observed in this phase.
- For event 5, when the current and voltage waveform demonstrated in Figure A5 is examined, it is observed that there is voltage sag in phases a and b, and the current in these phases increases. While the proposed algorithm classifies the voltage sag direction as DS, the fault type is determined as LLGF.
- For event 6, Figure A6 shows the voltage and current waveform recorded by the PQ analyzer. As can be seen from Figure A6, it is encountered with voltage sag in three phases, and the excessive current is drawn from three phases. The presented algorithm detects the voltage sag relative location and fault type as DS and LLLGF, respectively.
- For events 7–8, when the voltage and the current waveforms represented in Figures A7 and A8 are analyzed, although there is voltage collapse in some phases, it has been observed that there is no increase in the currents drawn from these phases. The algorithm detects the direction of voltage sag as US.

For the events investigated above, algorithm results are verified by voltage and current waveform recorded by the PQ.

Table 3. Rules of determination of fault type.

SR ₁ : if ($V_{1min} \leq 0.9$ and $V_{2max} \geq 1.1$ and $V_{3min} > 0.9$ and $V_{3max} < 1.1$) then SLGF
SR ₂ : if ($V_{1min} \leq 0.9$ and $V_{2max} < 1.1$ and $V_{2min} > 0.9$ and $V_{3max} \geq 1.1$) then SLGF
SR ₃ : if ($V_{1min} > 0.9$ and $V_{1max} < 1.1$ and $V_{2min} \leq 0.9$ and $V_{3max} \geq 1.1$) then SLGF
SR ₄ : if ($V_{1min} > 0.9$ and $V_{1max} < 1.1$ and $V_{2max} \geq 1.1$ and $V_{3min} \leq 0.9$) then SLGF
SR ₅ : if ($V_{1max} \geq 1.1$ and $V_{2min} \leq 0.9$ and $V_{3min} > 0.9$ and $V_{3max} < 1.1$) then SLGF
SR ₆ : if ($V_{1max} \geq 1.1$ and $V_{2min} > 0.9$ and $V_{2max} < 1.1$ and $V_{3min} < 0.9$) then SLGF
SR ₇ : if ($V_{1min} \leq 0.9$ and $V_{2min} > 0.9$ and $V_{2max} < 1.1$ and $V_{3min} > 0.9$ and $V_{3max} < 1.1$) then SLGF
SR ₈ : if ($V_{1min} > 0.9$ and $V_{1max} < 1.1$ and $V_{2min} \leq 0.9$ and $V_{3min} > 0.9$ and $V_{3max} < 1.1$) then SLGF
SR ₉ : if ($V_{1min} > 0.9$ and $V_{1max} < 1.1$ and $V_{2min} > 0.9$ and $V_{2max} < 1.1$ and $V_{3min} \leq 0.9$) then SLGF
SR ₁₀ : if ($V_{1min} \leq 0.9$ and $V_{2max} \geq 1.1$ and $V_{3max} \geq 1.1$) then SLGF
SR ₁₁ : if ($V_{1max} \geq 1.1$ and $V_{2min} \leq 0.9$ and $V_{3max} \geq 1.1$) then SLGF
SR ₁₂ : if ($V_{1max} \geq 1.1$ and $V_{2max} \geq 1.1$ and $V_{3min} \leq 0.9$) then SLGF
SR ₁₃ : if ($V_{1min} \leq 0.9$ and $V_{2min} \leq 0.9$ and $V_{3max} < 1.1$ and $V_{3min} > 0.9$) then LLF
SR ₁₄ : if ($V_{1min} \leq 0.9$ and $V_{2min} > 0.9$ and $V_{2max} < 1.1$ and $V_{3min} \leq 0.9$) then LLF
SR ₁₅ : if ($V_{1min} > 0.9$ and $V_{1max} < 1.1$ and $V_{2min} \leq 0.9$ and $V_{3min} \leq 0.9$) then LLF
SR ₁₆ : if ($V_{1min} \leq 0.9$ and $V_{2min} \leq 0.9$ and $V_{3max} \geq 1.1$) then LLGF
SR ₁₇ : if ($V_{1min} \leq 0.9$ and $V_{2max} \geq 1.1$ and $V_{3min} \leq 0.9$) then LLGF
SR ₁₈ : if ($V_{1max} \geq 1.1$ and $V_{2min} \leq 0.9$ and $V_{3min} \leq 0.9$) then LLGF
SR ₁₉ : if ($V_{1min} \leq 0.9$ and $V_{2min} \leq 0.9$ and $V_{3min} \leq 0.9$) then LLLGF

Table 4. Example of data provided by PQMS.

Event ID	Event Direction	Fault Type	V-I Data
1	DS	SLGF	Figure A1
2	DS	SLGF	Figure A2
3	DS	SLGF	Figure A3
4	DS	SLGF	Figure A4
5	DS	LLGF	Figure A5
6	DS	LLLGF	Figure A6
7	US	_____	Figure A7
8	US	_____	Figure A8

3. Simulation Study

The proposed algorithm also is tested in a radial power system shown in Figure 5. The power system has nine buses, where B1 is the 154 kV transmission system bus, and the remaining busbar is a 34.5 kV bus in the distribution system. Moreover, it has four monitoring points. To observe the voltage sag, faults (SLGF, LLGF, LLLGF, and LLF) are applied to F1 and F2 points. The proposed algorithm determines the voltage sag and fault type, as shown in Table 5. When the simulation results are investigated, the proposed algorithm correctly determines the voltage sag location and fault type in all monitoring points.

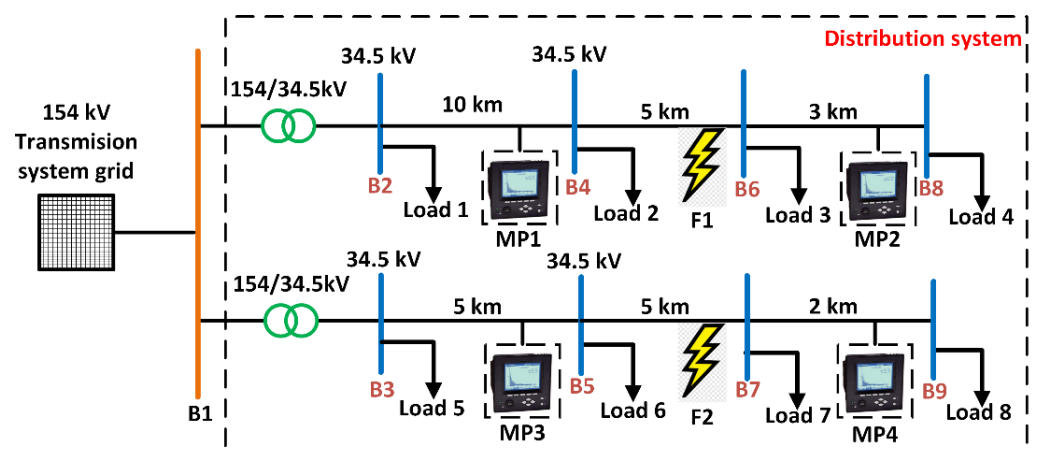
**Figure 5.** Test system.

Table 5. Simulation results.

Fault Location	Monitoring Point			
	MP1	MP2	MP3	MP4
F1	Downstream	Upstream	Upstream	Upstream
F2	Upstream	Upstream	Downstream	Upstream

4. Conclusions

In this study, the novel algorithm is proposed to detect the voltage sag relative location using real voltage and current data provided by PQMS in an actual distribution company. Moreover, the algorithm is integrated into the PQMS of the distribution company. The proposed algorithm is tested in nine bus power systems and correctly determines voltage sag relative location and fault type in all monitoring points. In addition, the performance of the algorithm is approved by voltage and current waveform recorded by the PQ analyzer. This algorithm can also be implemented in the PQMS of other distribution system companies that use Inavitas as a PQMS. On the other hand, if the network topology is integrated into PQMS, the exact location of the voltage sag can be determined with the help proposed algorithm. For future studies, the threshold for rules can be defined by the artificial intelligence method.

Author Contributions: Conceptualization, Y.Y. and T.U.; methodology, Y.Y., K.Ç.B. and A.T.; software, Y.Y. and T.U.; validation, Y.Y., Y.T., and A.T.; writing—original draft preparation, Y.Y. and T.U.; writing—review and editing, A.T., Y.T., J.M.G. and C.-L.S.; supervision, K.Ç.B. and J.M.G. All authors have read and agreed to the published version of the manuscript.

Funding: This work was supported by The Scientific and Technological Research Council of Turkey BIDEB-2214-A International Research Fellowship Programme for PhD Students. The work of Chun-Lien Su was funded by the Ministry of Science and Technology of Taiwan under Grant MOST 110-2221-E-992-044-MY3.

Acknowledgments: The authors would like to thank ENDOKS and KCETAS companies.

Conflicts of Interest: The authors declare no conflict of interest.

Appendix A

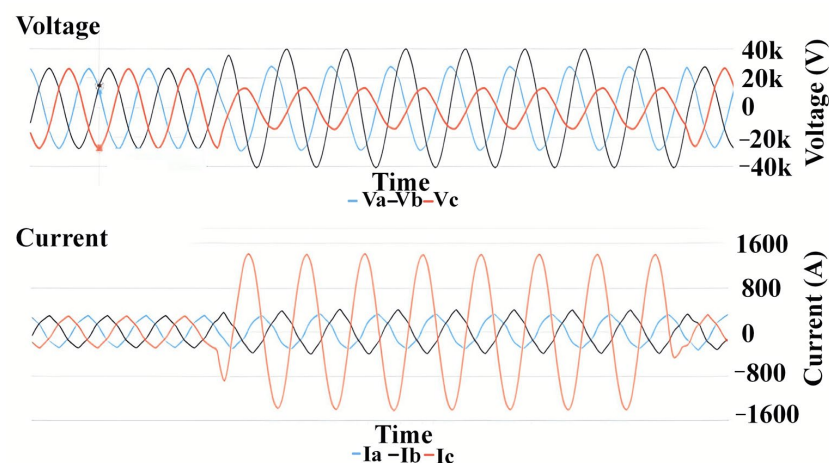


Figure A1. Current and voltage waveform recorded by PQ analyzer during the voltage sag for event 1.

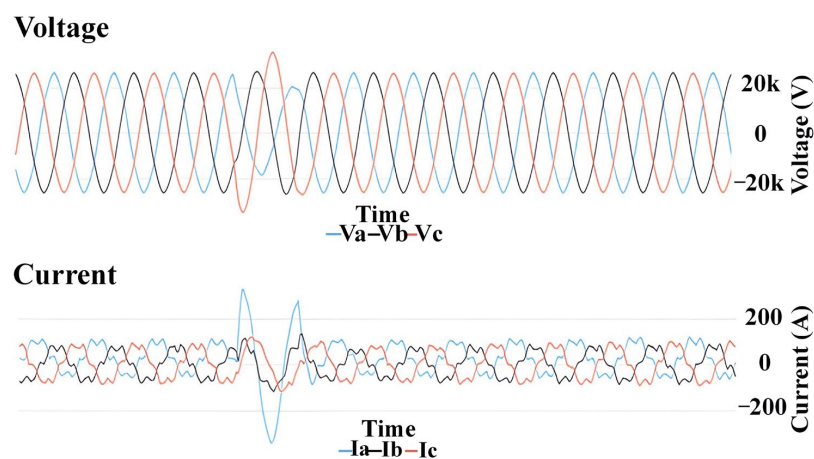


Figure A2. Current and voltage waveform recorded by PQ analyzer during the voltage sag for event 2.

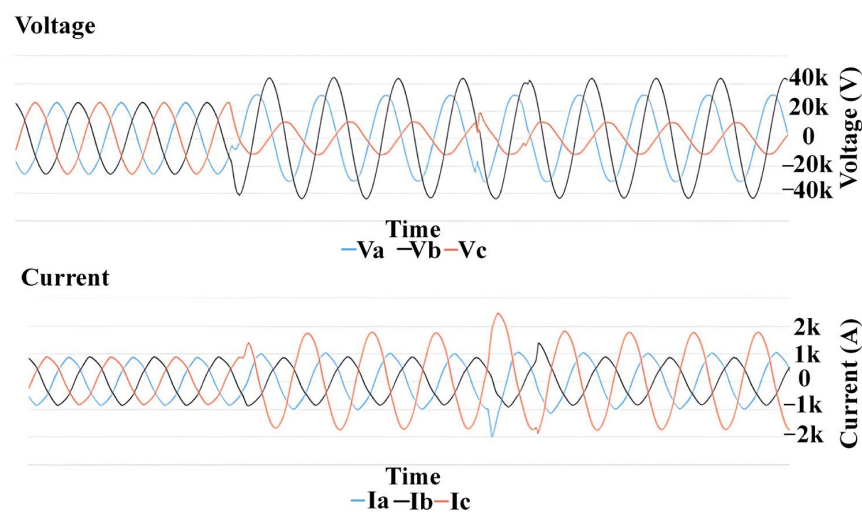


Figure A3. Current and voltage waveform recorded by PQ analyzer during the voltage sag for event 3.

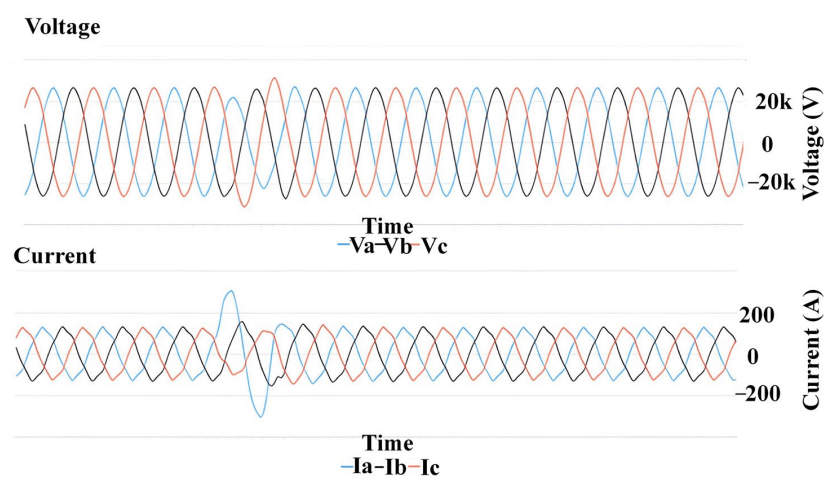


Figure A4. Current and voltage waveform recorded by PQ analyzer during the voltage sag for event 4.

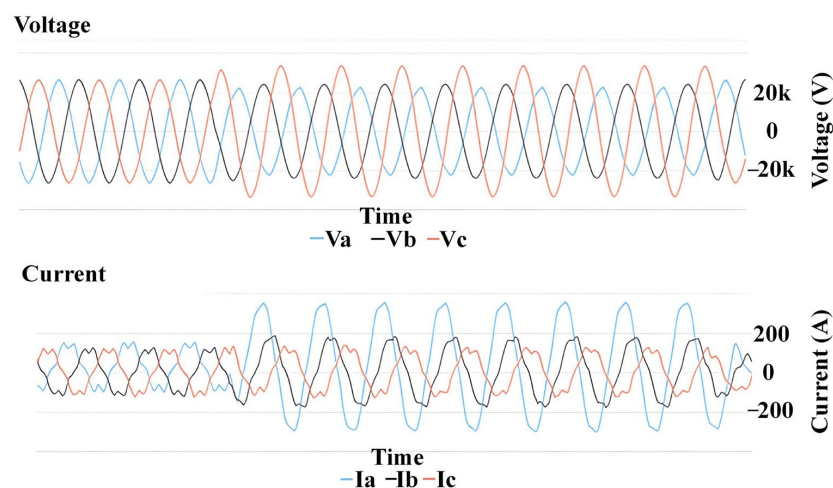


Figure A5. Current and voltage waveform recorded by PQ analyzer during the voltage sag for event 5.

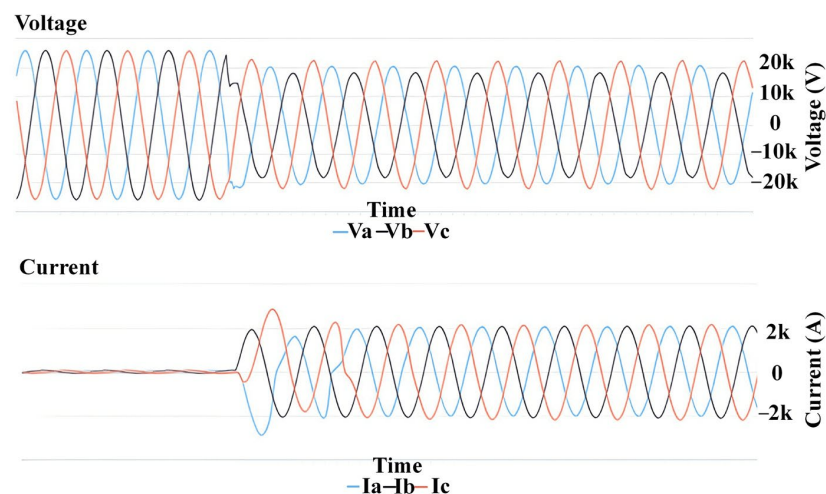


Figure A6. Current and voltage waveform recorded by PQ analyzer during the voltage sag for event 6.

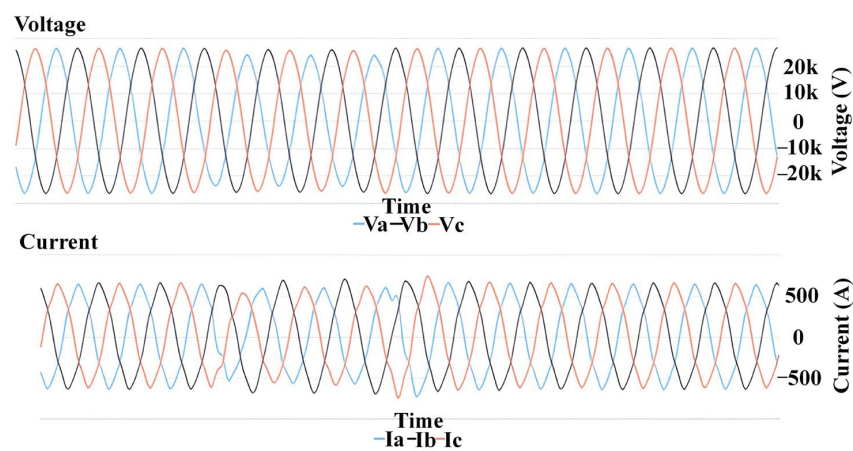


Figure A7. Current and voltage waveform recorded by PQ analyzer during the voltage sag for event 7.

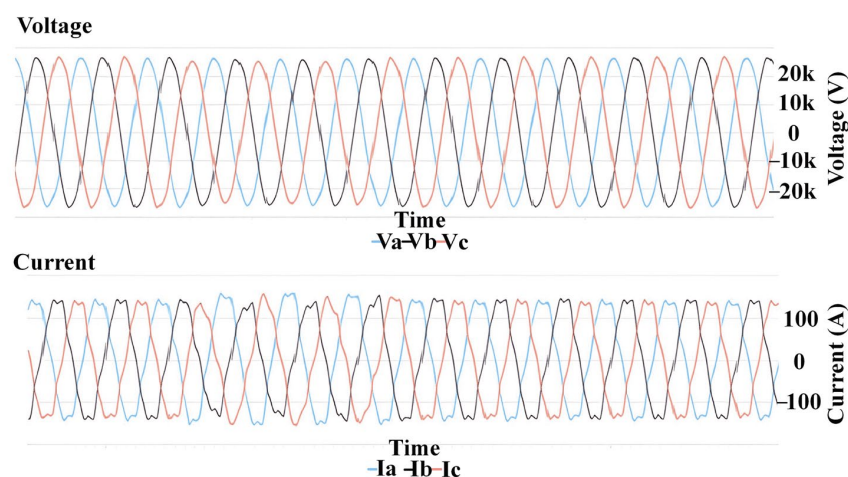


Figure A8. Current and voltage waveform recorded by PQ analyzer during the voltage sag for event 8.

References

1. IEEE. *IEEE Recommended Practice for Monitoring Electric Power Quality*; IEEE: Piscataway, NJ, USA, 1995; Volume 2019, ISBN 978-0-7381-5940-9.
2. Hartings, R.; Andersson, T.; Sveanät, V.; Ceder, Å. *Test and Evaluation of Voltage Dip Immunity*; STRI: Bingley, UK, 2002.
3. McGranaghan, M.F.; Mueller, D.R.; Samotyj, M.J. Voltage Sags in Industrial Systems. *IEEE Trans. Ind. Appl.* **1993**, *29*, 397–403. [\[CrossRef\]](#)
4. Heine, P.; Pohjanheimo, P.; Lehtonen, M.; Lakervi, E. A Method for Estimating the Frequency and Cost of Voltage Sags. *IEEE Trans. Power Syst.* **2002**, *17*, 290–296. [\[CrossRef\]](#)
5. Samotyj, M.J.; Mielczarski, W.; Wasiluk-Hassa, M.M. Electric Power for the Digital Age. *Proc. Int. Conf. Harmon. Qual. Power ICHQP 2002*, *1*, 276–282. [\[CrossRef\]](#)
6. Yi, T.; Jie, H.; Hao, L.; Lei, W. Method for Voltage Sag Source Location Based on the Internal Resistance Sign in a Single-Port Network. *IET Gener. Transm. Distrib.* **2016**, *10*, 1720–1727. [\[CrossRef\]](#)
7. Meral, M.E.; Teke, A.; Bayindir, K.C.; Tumay, M. Power Quality Improvement with an Extended Custom Power Park. *Electr. Power Syst. Res.* **2009**, *79*, 1553–1560. [\[CrossRef\]](#)
8. Yalman, Y.; Celik, O.; Tan, A.; Bayindir, K.C.; Cetinkaya, U.; Yesil, M.; Akdeniz, M.; Tinajero, G.D.A.; Chaudhary, S.K.; Guerrero, J.M.; et al. Impacts of Large-Scale Offshore Wind Power Plants Integration on Turkish Power System. *IEEE Access* **2022**, *10*, 83265–83280. [\[CrossRef\]](#)
9. De Santis, M.; Noce, C.; Varilone, P.; Verde, P. Analysis of the Origin of Measured Voltage Sags in Interconnected Networks. *Electr. Power Syst. Res.* **2018**, *154*, 391–400. [\[CrossRef\]](#)
10. Moradi, M.H.; Mohammadi, Y. Voltage Sag Source Location: A Review with Introduction of a New Method. *Int. J. Electr. Power Energy Syst.* **2012**, *43*, 29–39. [\[CrossRef\]](#)
11. Parsons, A.C.; Grady, W.M.; Powers, E.J.; Soward, J.C. A Direction Finder for Power Quality Disturbances Based upon Disturbance Power and Energy. *IEEE Trans. Power Deliv.* **2000**, *15*, 1081–1086. [\[CrossRef\]](#)
12. Kong, W.; Dong, X.; Chen, Z. Voltage Sag Source Location Based on Instantaneous Energy Detection. *Electr. Power Syst. Res.* **2008**, *78*, 1889–1898. [\[CrossRef\]](#)
13. Li, C.; Tayjasant, T.; Xu, W.; Liu, X. Method for Voltage-Sag-Source Detection by Investigating Slope of the System Trajectory. *IEE Proc. Commun.* **2003**, *150*, 367–372. [\[CrossRef\]](#)
14. Hamzah, N.; Mohamed, A.; Hussain, A. A New Approach to Locate the Voltage Sag Source Using Real Current Component. *Electr. Power Syst. Res.* **2004**, *72*, 113–123. [\[CrossRef\]](#)
15. Moradi, M.H.; Mohammadi, Y. A New Current-Based Method for Voltage Sag Source Location Using Directional Overcurrent Relay Information. *Int. Trans. Electr. Energy Syst.* **2013**, *23*, 270–281. [\[CrossRef\]](#)
16. Polajžer, B.; Štumberger, G.; Dolinar, D. Detection of Voltage Sag Sources Based on the Angle and Norm Changes in the Instantaneous Current Vector Written in Clarke's Components. *Int. J. Electr. Power Energy Syst.* **2015**, *64*, 967–976. [\[CrossRef\]](#)
17. Polajžer, B.; Štumberger, G.; Seme, S.; Dolinar, D. Detection of Voltage Sag Sources Based on Instantaneous Voltage and Current Vectors and Orthogonal Clarke's Transformation. *IET Gener. Transm. Distrib.* **2008**, *2*, 219–226. [\[CrossRef\]](#)
18. Blanco-Solano, J.; Petit-Suárez, J.F.; Ordóñez-Plata, G. Methodology for Relative Location of Voltage Sag Source Using Voltage Measurements Only. *DYNA* **2015**, *82*, 94–100. [\[CrossRef\]](#)
19. Leborgne, R.; Karlsson, D. Voltage Sag Source Location Based on Voltage Measurements Only. *Electr. Power Qual. Util.* **2008**, *XIV*, 25–30.

20. Tayjasanant, T.; Li, C.; Xu, W. A Resistance Sign-Based Method for Voltage Sag Source Detection. *IEEE Trans. Power Deliv.* **2005**, *20*, 2544–2551. [[CrossRef](#)]
21. Mohammadi, Y.; Leborgne, R.C. A New Approach for Voltage Sag Source Relative Location in Active Distribution Systems with the Presence of Inverter-Based Distributed Generations. *Electr. Power Syst. Res.* **2020**, *182*, 106222. [[CrossRef](#)]
22. Mohammadi, Y.; Leborgne, R.C. Relative Location of Voltage Sags Source at the Point of Common Coupling of Constant Power Loads in Distribution Systems. *Int. Trans. Electr. Energy Syst.* **2020**, *30*, 1–15. [[CrossRef](#)]
23. Yalman, Y.; Uyanık, T.; Athi, İ.; Tan, A.; Bayındır, K.Ç.; Karal, Ö.; Golestan, S.; Guerrero, J.M. Prediction of Voltage Sag Relative Location with Data-Driven. *Energies* **2022**, *15*, 6641. [[CrossRef](#)]
24. Mohammadi, Y.; Salarpour, A.; Chouhy Leborgne, R. Comprehensive Strategy for Classification of Voltage Sags Source Location Using Optimal Feature Selection Applied to Support Vector Machine and Ensemble Techniques. *Int. J. Electr. Power Energy Syst.* **2020**, *124*, 106363. [[CrossRef](#)]
25. Kazemi, A.; Mohamed, A.; Shareef, H.; Raihi, H. Accurate Voltage Sag-Source Location Technique for Power Systems Using GACp and Multivariable Regression Methods. *Int. J. Electr. Power Energy Syst.* **2014**, *56*, 97–109. [[CrossRef](#)]
26. Kazemi, A.; Mohamed, A.; Shareef, H. Tracking the Voltage Sag Source Location Using Multivariable Regression Model. *Int. Rev. Electr. Eng.* **2011**, *6*, 1853–1861.
27. Liao, H.; Anani, N. Fault Identification-Based Voltage Sag State Estimation Using Artificial Neural Network. *Energy Procedia* **2017**, *134*, 40–47. [[CrossRef](#)]
28. Turović, R.; Dragan, D.; Gojić, G.; Petrović, V.B.; Gajić, D.B.; Stanisavljević, A.M.; Katić, V.A. An End-to-End Deep Learning Method for Voltage Sag Classification. *Energies* **2022**, *15*, 2898. [[CrossRef](#)]
29. Liao, H.; Milanovic, J.V.; Rodrigues, M.; Shenfield, A. Voltage Sag Estimation in Sparsely Monitored Power Systems Based on Deep Learning and System Area Mapping. *IEEE Trans. Power Deliv.* **2018**, *33*, 3162–3172. [[CrossRef](#)]
30. Borges, F.A.S.; Rabelo, R.A.L.; Fernandes, R.A.S.; Araujo, M.A. Methodology Based on Adaboost Algorithm Combined with Neural Network for the Location of Voltage Sag Disturbance. *Proc. Int. Jt. Conf. Neural Netw.* **2019**, 1–7. [[CrossRef](#)]
31. Deng, Y.; Liu, X.; Jia, R.; Huang, Q.; Xiao, G.; Wang, P. Sag Source Location and Type Recognition via Attention-Based Independently Recurrent Neural Network. *J. Mod. Power Syst. Clean Energy* **2021**, *9*, 1018–1031. [[CrossRef](#)]
32. Lv, G.; Sun, W. Voltage Sag Source Location Based on Pattern Recognition. *J. Energy Eng.* **2013**, *139*, 136–141. [[CrossRef](#)]
33. Liu, J.; Song, H.; Zhou, L. Identification and Location of Voltage Sag Sources Based on Multi-Label Random Forest. In Proceedings of the IEEE Sustainable Power and Energy Conference (iSPEC), Beijing, China, 21–23 November 2019; pp. 2025–2030. [[CrossRef](#)]
34. Enerji Yönetim Sistemi | Inavitas (EMS). Available online: <https://www.inavitas.com/tr/> (accessed on 15 August 2022).